WARM ROTATING NUCLEI: DAMPING MECHANISMS AND THE ORDER-TO-CHAOS TRANSITION*

S. Leoni[a], G. Benzoni[a], A. Bracco[a], N. Blasi[a], F. Camera[a] C. Grassi[a], B. Million[a], A. Paleni[a], M. Pignanelli[a], E. Vigezzi[a] O. Wieland[a], M. Matsuo[b], T. Døssing[c], B. Herskind[c] G.B. Hagemann[c], J. Wilson[c], A. Maj[d], M. Kmiecik[d] G. Lo Bianco[e], C.M. Petrache[e], M. Castoldi[f], A. Zucchiati[f] G. De Angelis[g], D. Napoli[g], P. Bednarczyk[d,h], and D. Curien[i]

[a]Dipartimento di Fisica and INFN Sez. Milano, Italy
[b]Graduate School of Science and Technology, Niigata University, Japan
[c]The Niels Bohr Institute, Copenhagen, Denmark
[d]Institute of Nuclear Physics, Polish Academy of Sciences, Kraków, Poland
[e]Dipartimento di Fisica Universitá di Camerino and INFN sez. Perugia, Italy
[f]INFN sez. Genova, Genova, Italy
[g]Laboratori Nazionali di Legnaro, Italy
[h]GSI Darmstadt, Germany
[i]Institut de Recherches Subatomiques, Strasbourg, France

(Received November 30, 2004)

The γ-decay in the quasi-continuum is used as a probe of nuclear structure properties in thermally excited nuclei. The experimental analysis is performed on high-statistics EUROBALL data on ^{163}Er, and the results are compared to band mixing calculations for this nucleus. Two topics are investigated. First, a direct experimental measurement of the rotational and compound damping width ($\Gamma_{\rm rot}$ and Γ_μ) is given. From a line-shape analysis of γ–γ coincidence spectra values of 200 and 20 keV are obtained for $\Gamma_{\rm rot}$ and Γ_μ, respectively, in the spin region $I \approx 30$–$40\hbar$, in good agreement with theory. Secondly, the validity of the selection rules associated with the K-quantum number are investigated as a function of the internal energy U above yrast. K-selection rules are found to be obeyed in the decay along discrete unresolved rotational bands up to $U \approx 1.2$ MeV, while in the interval $U \approx 1.2$–2.5 MeV, where the order-to-chaos transition is expected to take place, selection rules are found to be only partially valid.

PACS numbers: 21.10.Pc, 21.10.Re, 21.60.Ev, 21.60.Ka

* Presented at the XXXIX Zakopane School of Physics — International Symposium "Atomic Nuclei at Extreme Values of Temperature, Spin and Isospin", Zakopane, Poland, August 31–September 5, 2004.

1. Introduction

The γ-decay from rapidly rotating warm nuclei produced in heavy-ion fusion evaporation reactions can be used to investigate nuclear structure properties at finite temperature [1]. It is found that, already at internal energies $U \approx 1$ MeV above yrast, the nuclear rotation becomes damped, due to the mixing of closely spaced levels via the two-body residual interaction. As a consequence, the rotational E2 strength fragments over a number of states, acquiring a width $\Gamma_{\rm rot}$ (the rotational damping width), which depends on the thermal energy. Above $U \approx 2.5$ MeV a fully chaotic regime is reached, as shown in Ref. [2,3]. The study of rotational damping becomes, therefore, instrumental to shed light on the order-to-chaos transition undertaken by the atomic nucleus as the thermal energy increases.

The properties of rotational damping have been largely investigated as function of atomic mass, deformation and intrinsic nuclear configuration [1] by the use of ad-hoc experimental techniques based on statistical fluctuation and line-shape analysis of the ridge-valley structure observed in γ–γ coincidence spectra [4, 5]. In fact, while the ridges carry information from the decay along discrete rotational bands up to ≈ 1 MeV above yrast, the valley region mostly collects contributions from the more excited strongly interacting bands (rotational damping regime). In addition, the development of cranked shell model calculation including also a residual two-body force [6] has provided a microscopic description of nuclear levels and E2 transitions in the thermally excited nucleus, allowing to study in more detail the properties of rapidly rotating nuclei with internal energies up to a few MeV above yrast.

In the present paper we will focus on two different topics, basing our discussion on an high-statistics data set on the nucleus ^{163}Er, taken with the EUROBALL array. First, we will present a direct experimental measurement of the rotational and compound damping widths $\Gamma_{\rm rot}$ and Γ_μ, which so far have been estimated only indirectly. While $\Gamma_{\rm rot}$ plays a central role mostly in connection with the nuclear rotation, the compound damping width Γ_μ enters the description of all basic nuclear phenomena at finite temperature (*e.g.* giant resonances [7]), being a measure of the mixing of the intrinsic mean-field configurations under the action of a two-body residual interaction. The analysis technique is based on the study of the line-shape of the quasi-continuum ridge-valley structure (typical of warm rotational nuclei) observed in γ–γ coincidence spectra. Such an analysis makes use of an analytic function which takes into account the complex nature of the B(E2) strength distribution, that is found to carry information on both $\Gamma_{\rm rot}$ and Γ_μ [8].

As a second topic we will discuss the violation of selection rules associated with the K-quantum number (the projection of aligned nucleonic angular momentum on the symmetry axis), as a function of thermal energy U. This allows to investigate the transition between order and chaos undertaken by the atomic nucleus with increasing U [2]. The analysis is made by comparing the γ-decay flows feeding low-K and high-K discrete bands in terms of statistical fluctuations of the counts collected in the corresponding γ–γ-coincidence spectra. The experimental findings will be compared to cranked shell model calculations for the specific nucleus, including both the residual interaction and a term taking into account the angular momentum carried by the K-quantum number [9].

2. The experiment

The experiment was performed using the EUROBALL array at the IReS Laboratory (France), employing the reaction ^{18}O + ^{150}Nd, at E_{beam} = 87, 93 MeV. The ^{150}Nd target was made of a stack of two thin foils for a total thickness of 740 μg/cm^2. The corresponding maximum angular momentum reached in the reaction has been calculated to be 40 and 45 $\hbar$, respectively. Energy-dependent time gates on the Ge time signals were used to suppress background from neutrons. A total of $\approx 3\times 10^9$ events of triple and higher Ge-folds were finally obtained, with ^{162,163}Er as main evaporation residua. The data have been sorted into a number of matrices in coincidence with specific γ-transitions of the ^{163}Er nucleus. The matrix collecting the entire decay flow of ^{163}Er (named *total*) has been constructed by gating on the three cleanest low spin transitions. In addition, seven matrices gated by transitions belonging to the low-K bands ($K = 5/2$) labeled A, B, E and F in Ref. [10], and by the high-K bands ($K = 19/2$) labeled K1, K2 and K4 in Ref. [10] have been sorted, together with their corresponding two-dimensional (2D) background. For each 2D spectrum all known peak–peak and peak–background coincidences have been subtracted using the Radware software [11]. The separately gated matrices have also been added together in one *low–K* (A+B+E+F) and one *high-K* (K1+K2+K4) matrix. In the case of the experimental measurement of the compound and rotational damping widths $\Gamma_{\rm rot}$ and Γ_μ (discussed in Section 3) a correction for the detector efficiency has also been applied to the data.

3. Experimental measurement of the damping widths $\Gamma_{\rm rot}$ and Γ_μ

The analysis method discussed here [12] allows, for the first time, to directly extract the rotational and compound damping widths $\Gamma_{\rm rot}$ and Γ_μ from the data. This method has been developed following a detailed study

of the strength function for two consecutive γ-transitions, as obtained from cranked shell model calculation (CSM) for the ^{163}Er nucleus [9]. In fact, as shown in figure 1(a) for the excited states 11 to 100 at spin $I = 40, 41\hbar$, the projection of the E2 strength distribution for two consecutive transitions, on the E_{γ_1}–E_{γ_2} axis, shows clearly a two-component structure. This distribution can be approximated by an analytic function made by the superposition of two Gaussians of width $\Gamma_{\rm wide}$ and $\Gamma_{\rm nar}$ (solid line in figure 1(a)). As discussed in Ref. [8], it is found that the wide width $\Gamma_{\rm wide}$ is $\approx \sqrt{2}\Gamma_{\rm rot}$, while the narrow width $\Gamma_{\rm nar}$ is $\approx 2\Gamma_{\mu}$. Such two-component structure contributes also to the line-shape of two and higher fold γ-coincidence spectra from multiple steps of E2 decay, as shown in panel 1(b) for a calculated spectrum of ^{163}Er, relative to levels 11–100 in the spin range 28–40 $\hbar$. A parameterized spectrum function is introduced, which allows to directly extract the damping widths $\Gamma_{\rm rot}$ and Γ_{μ} from the multiple γ-decay strength distribution (solid line in figure 1(b)). This function is an extension of the analytic two-component function, shown in figure 1(a), to multiple steps of E2 γ-decay. It is found that the calculated multiple steps pure E2 spectrum (histogram in panel 1(b)) is well accounted for by the analytic approximation (solid line), at variance from the case in which the narrow component is neglected (dashed line).

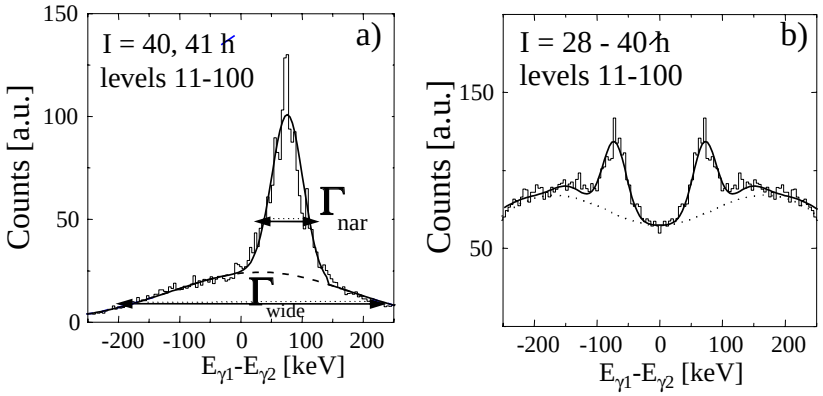

Fig. 1. Panel (a): projection on the E_{γ_1}–E_{γ_2} axis of the E2 strength function for two consecutive E2 γ-rays, calculated microscopically for the levels 11–100 at spin $I = 40, 41\hbar$ for ^{163}Er [9]. The full drawn line represents the analytic two-component function containing a wide and a narrow Gaussian component of width $\Gamma_{\rm wide}$ and $\Gamma_{\rm nar}$, respectively. Panel (b): projection on the E_{γ_1}–E_{γ_2} axis of a spectrum microscopically calculated for multiple steps of E2 decay, for the levels 11–100 of ^{163}Er, in the spin range 28 to 40$\hbar$. The full drawn line is the parametrized spectrum for multiple steps, with $\Gamma_{\rm rot} = 180$ keV and $\Gamma_{\rm nar} = 44$ keV, while the dashed line has no narrow component and a width $\Gamma_{\rm rot} = 150$ keV.

The method has been tested on γ-coincidence spectra obtained by a Monte Carlo code which simulates the γ-cascades via the competition between E1 and E2 transitions, at each step of the decay [13]. The simulations make use of the levels and E2 transition probabilities microscopically calculated for the ^{163}Er nucleus [9]. In addition, in order to take into account the difference in K quantum number between initial and final states, an exponential quenching factor is included, similar to that employed for the analysis of the E1 decay-out from isomeric states [14, 15]. Each γ-cascade is started from initial values of internal energy and spin randomly chosen from a two-dimensional entry distribution of Gaussian shape, with centroids and widths reproducing the experimental conditions of the ^{163}Er experiment under study (*i.e.* $\langle U\rangle$ = 4 MeV, FWHM$_U$ = 4 MeV, $\langle I\rangle$ = 44 $\hbar$, FWHM$_I$ = 20 $\hbar$). Examples of a 60 keV wide cuts on the simulated matrices collecting the E2 strength from pure discrete rotational bands (bottom) and damped rotational states (top) are shown in figure 2(b). The projections are taken across the $E_{\gamma_1} = E_{\gamma_2}$ diagonal, at the average transition energy $\langle E_\gamma\rangle$ = 960 keV, corresponding to spin $I = 32\hbar$. In both cases a ridge-valley structure is clearly visible, with a separation between the two most inner ridges equal to $8\hbar^2/J^{(2)}$, $J^{(2)}$ being the dynamic moment of inertia of the bands. As one can see, the damped spectrum is rather similar to the parametrized spectrum of figure 1(b) and to the experimental data of panel 2(a), while it differs from the spectrum associated with discrete bands, which displays sharp ridges with FWHM $\approx$ 20 keV. The smooth line superposed on the damped spectrum (both in simulation and data) is the best fit obtained using the analytic parametrization [12], which gives values of $\Gamma_{\rm nar}$ and $\Gamma_{\rm rot}$ of the order of 40 and 200 keV, respectively. The results are shown in figure 2(c) and (d) in comparison with the values deduced directly from the calculated CSM bands for the low-lying levels ($n_b < 2$), for the levels 11 to 100 (with $\langle U\rangle \approx$1.4 MeV (solid line)), and for the levels 101 to 300 (with $\langle U\rangle \approx 2$ MeV (dashed line)). The analysis of the simulated damped spectrum agrees with the CSM prediction relative to the intermediate energy region, where the simulated γ-decay flow mostly goes at this spin interval. This supports the internal consistency of the present analysis technique.

The line-shape analysis technique has been applied to the *total*, *low-K* and *high-K* experimental 2D spectra of ^{163}Er, discussed in Section 2. The pure E2 rotational correlations have been isolated by subtracting the E1$\times$ E1 + E1$\times$ E2 + E2$\times$ E1 background components. These have been obtained assuming for the E1 spectrum the exponential shape $\sim E_\gamma^3 \exp(-E_\gamma/T)$, being $T \approx 0.45$ MeV the nuclear temperature [16, 17].

Figure 2(a) shows an example of a one-dimensional projection along the $E_{\gamma_1} = E_{\gamma_2}$ diagonal, 60 keV wide, at $\langle E_\gamma\rangle$ = 960 keV (corresponding to spin 32$\hbar$), taken on the *total* matrix. The rather smooth ridge-valley profile

is well reproduced by the analytic two-component function (full solid line), giving values of $\Gamma_{\rm nar}$ and $\Gamma_{\rm rot}$ of the order of 200 and 40 keV, respectively (figure 2(c) and (d)), in good agreement with both the CSM predictions and the results from the simulated spectra.

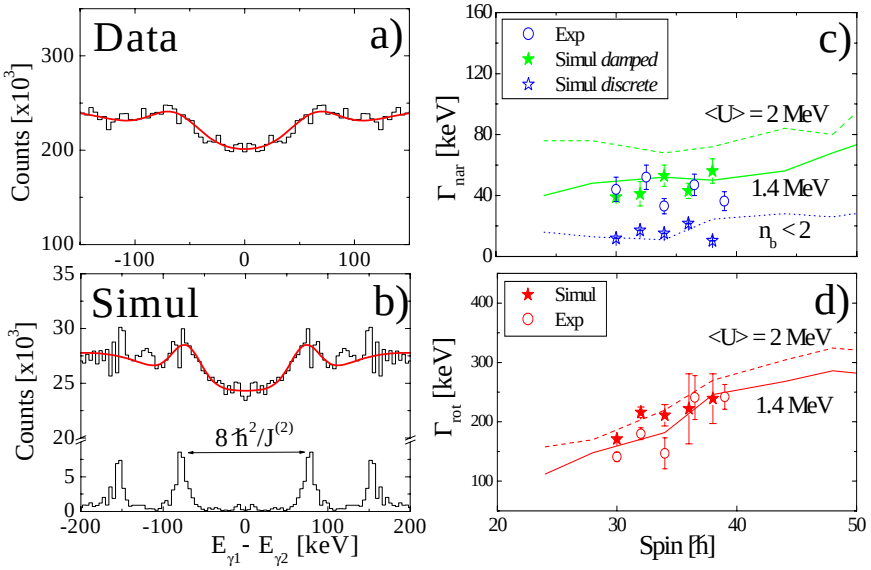

Fig. 2. (a): 60 keV wide projection on the E2 damped component of the *total* matrix of ^{163}Er, at $\langle E_\gamma \rangle = 960$ keV. The solid line superposed on the spectrum is the interpolation by the analytic two component function. Panel (b): projections on simulated spectra collecting the E2 strengths from discrete rotational bands (bottom) and damped transitions (top). The interpolation of the damped spectrum by the two component function is given by the solid line. Panels (c) and d) show values of $\Gamma_{\rm rot}$ and $\Gamma_{\rm nar}$, respectively. The lines refer to the values calculated directly from the CSM bands at different excitation energies: for $\langle U \rangle < 1$ MeV (in which case the bands branch-out to less than 2 final states, $n_b < 2$), $\langle U \rangle \approx 1.4$ MeV and $\langle U \rangle \approx 2$ MeV. The open (filled) stars refer to the values extracted from the simulated discrete (damped) spectra using the analytic parametrization. Finally, the circles refer to the experimental data.

The results from the analysis on the *low-K* and *high-K* matrices are shown in figure 3, in comparison with the corresponding low-K (K$\leq$8) and high-K ($K > 8$) predictions from CSM calculations. The extracted values of $\Gamma_{\rm rot}$ and $\Gamma_{\rm nar}$ are again, in average, of the order of 200 and 40 keV, respectively, in good agreement with the theoretical prediction relative to a colder decay-flow (*i.e.* $\langle U \rangle \approx 1.4$ MeV). A weak dependence of the damping width

on the K values is also observed, being $\Gamma_{\rm rot}$ almost 30% smaller for high-K states, as also shown in the calculations. This points to a difference in the mixing process between low-K and high-K states, which can be related to a partial conservation of the K-quantum number in the rotational damping region. This agrees with the theoretical prediction which show that high-K states maintain their rotational character even up to 1.5 MeV of excitation energies, namely in the region where rotational damping is otherwise largely dominating [9].

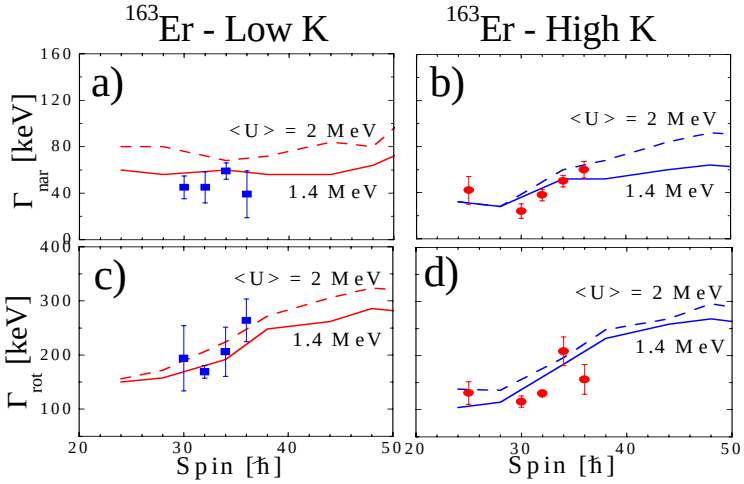

Fig. 3. Experimental values of $\Gamma_{\rm rot}$ and $\Gamma_{\rm nar}$ obtained from the line-shape analysis of low-K (panels (a) and (c)) and high-K (panel (b) and (d)) γ–γ spectra of ^{163}Er. Predictions from cranked shell model calculations at the average excitation energies of 1.4 and 2 MeV are shown by the solid and dashed lines, respectively.

4. The onset of chaos in warm nuclei

The validity of the selection rules on the K-quantum number are here investigated in the ^{163}Er nucleus, as a function of temperature. The aim is to study the order-to-chaos transition in the warm rotating nucleus, caused by the high level density and the residual interaction. In fact, as pointed out by Mottelson in Ref. [18], for a nuclear ordered system a complete set of single particle quantum numbers can be defined for each given states, resulting also in selection rules on the associated electromagnetic transitions. On the contrary, in a chaotic regime, due to the complex nature of every state, no precise definition of quantum numbers is possible (besides energy, spin and parity) and selection rules lose their validity.

The issue of K-validity has been previously addressed by studying the γ-decay from neutron resonances at internal energy $U \approx 8$ MeV and low spins [19, 20]. We will, instead, focus on high spin γ-transitions of quasi-continuum nature, which are probing the energy region extending up to $U \approx 4$ MeV internal energy, with particular emphasis on the lower energy region up to $\approx$ 2–3 MeV, where the order-to-chaos transition is expected to take place [2].

For this purpose, the γ–γ spectra measured in the ^{163}Er experiment (see section 2) have been studied with statistical analysis methods, which allow to determine the number $N_{\rm path}^{(2)}$ of decay paths in coincidence with specific low-K/high-K discrete bands [4] and the r correlation coefficient [5]. While $N_{\rm path}^{(2)}$ depends on both the level density and the rotational damping width, r measures the degree of sharing between decay paths through different sets of states and therefore the extent to which selection rules are obeyed during the decay. The fluctuations of counts in each channel of the 2D matrices, expressed as variance and covariance, have been evaluated and stored into 2D spectra [4]. Because each rotational E_γ-cascade on the average contributes one count in each $\frac{4\hbar^2}{J^{(2)}}$ interval, the statistical moments are evaluated over sectors of $\frac{4\hbar^2}{J^{(2)}} \times \frac{4\hbar^2}{J^{(2)}}$, corresponding to 60 keV$\times$60 keV intervals for rare earth nuclei around ^{163}Er.

First, the effective number of decay paths feeding into the gate-selected bands has been obtained using the expression

$$N_{\rm path}^{(2)} = \frac{N}{\frac{\mu_2}{\mu_1} - 1} \times P^{(2)}\,, \tag{1}$$

where N, μ_1 and μ_2 are the number of events, the first and second moments of the distribution of counts, while the $P^{(2)}$ factor takes into account the finite resolution of the detector system [4]. From the analysis of the ridge structure a total number of $\approx$ 20 paths is found for both *low-K* and *high-K* states, as shown in panel 4(a), while in the case of the *total* ^{163}Er matrix $\approx$ 45 discrete rotational bands are found, at heat energies below the onset of damping (triangles in figure 4(a)). On the contrary, the number of paths obtained from the valley region is found to depend significantly on the nuclear configuration (figure 4(b)), suggesting that in the region of strongly interacting bands the mixing process is different for high-K and low-K states.

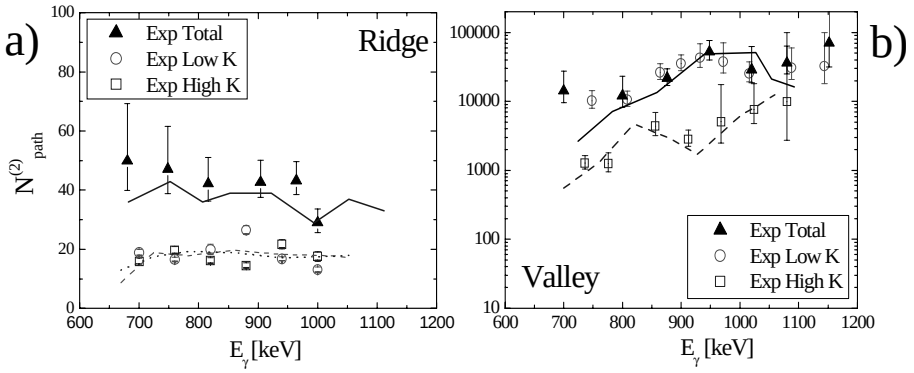

Fig. 4. Panel (a): The number $N^{(2)}_{\rm path}$ of decay paths extracted from the fluctuation analysis of the ridge structure of ^{163}Er. The open circles (squares) refer to γ–γ matrices gated by low-K (high-K) bands, while the full triangles give $N^{(2)}_{\rm path}$ from the total matrix. The corresponding values for simulated spectra are shown by dotted, dashed and full lines, respectively. Panel (b): The number $N^{(2)}_{\rm path}$ for the valley analysis is shown by open circles (squares) for low-K (high-K) gated spectra, while the full triangles give the results from the total γ–γ matrix. The dashed and solid lines refer to the prediction for total and high-K cascades, as obtained from simulated spectra.

Additional information on the mixing of states with different K-quantum numbers can be obtained from the correlations in fluctuations between spectra associated with low-K and high-K quantum numbers. Such correlations are expressed by the r correlation coefficient defined as [5]:

$$r(A,B) \equiv \frac{\mu_{2,\rm cov}(A,B)}{\sqrt{(\mu_2(A)-\tilde{\mu}_1(A))(\mu_2(B)-\tilde{\mu}_1(B))}}\,. \qquad (2)$$

Here, μ_2 denotes the second moment defined for the same region $N_{\rm ch}$, while $\mu_{2,\rm cov}(A,B) = \frac{1}{N_{\rm ch}}\sum_j (M_j(A)-\tilde{M}_j(A))((M_j(B)-\tilde{M}_j(B))$ is the covariance between the $M(A)$ and $M(B)$ spectra gated by transitions from two different bands, A and B. The sum is over a region spanning $N_{\rm ch}$ channels in a two-dimensional 60 keV$\times$60 keV window, and $\tilde{M}$ denotes an average reference spectrum, which can be, for example, a numerical smoothed approximation to the 2D spectrum. In the previous equation, the first moment $\tilde{\mu}_1$ is the average of M over the region $N_{\rm ch}$.

The average values of the r coefficient obtained from the analysis of the ridge and valley structures of ^{163}Er are shown by symbols in figure 5. In each panel the solid lines indicate the two opposite limits expected in the

case of a complete conservation of selection rules ($r = 0$) and of a compound nucleus regime ($r = 1$). In the case of the ridge analysis, r is found to be of the order of 0.2 for configurations with similar low-K values (panel 5(a)), while it is ≈0 for combinations of low-K and high-K spectra (panel 5(b)). This means that there are basically no cross-transitions between the ≈ 20 bands feeding high-K states and the ≈ 20 bands feeding low-K states. For the valley fluctuations, the correlation coefficient is still of the order of 0.2, but it increases with increasing E_γ in the case of low-K *versus* high-K. The numbers of paths in the valley gated by low-K and high-K bands also approach each other, as shown in figure 4(b). Both results suggest a weakening of selection rules associated with the K-quantum number with increasing rotational frequency and internal excitation energy.

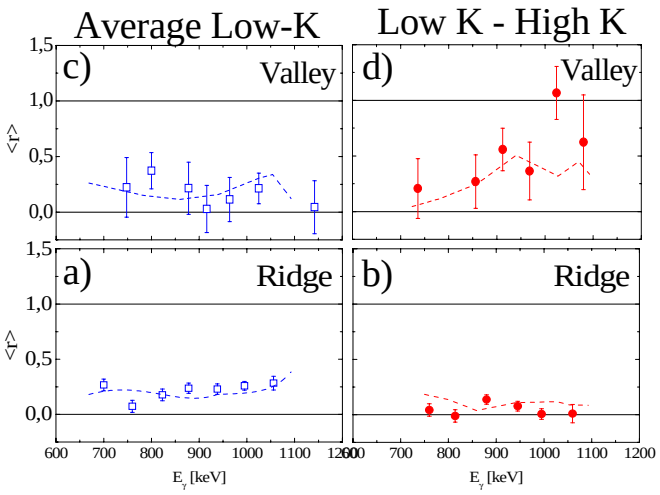

Fig. 5. The r coefficient obtained from the ridge (bottom) and valley (top) structures of ^{163}Er. The experimental data are shown by symbols, while the dashed lines refer to simulated spectra. The left column shows results obtained by averaging over pairs of γ–γ spectra gated by low-K configurations, while the analysis of *low-K versus high-K* matrices is shown in the right part.

The experimental values of $N^{(2)}_{\rm path}$ and r have been compared to a similar analysis on simulated γ–γ spectra [13]. The calculated matrices have been constructed by a Monte Carlo code which uses as input the band mixing calculations of Ref. [9], previously discussed in Section 3. The model predicts the onset of K-mixing at $U \approx 1.5$ MeV, while the statistical limit of strong K-mixing is approached only above 2.5 MeV.

The results obtained by the statistical analysis of the simulated data both for $N^{(2)}_{\rm path}$ and r are shown by lines in figure 4 and 5, respectively. In

agreement with the data, the calculation give a similar number of paths ($\approx$ 20) in the case of the ridges (figure 4(a)), while a clear difference in $N^{(2)}_{\rm path}$ is observed between low-K and high-K gated spectra up to $\approx$ 1 MeV (*i.e.* $I \approx 38\ \hbar$ and $U \approx 2$ MeV). The two quantities tend, instead, to converge at higher energies. This can be understood in terms of the onset of K-mixing, described above. In this lower energy region, not only the level density for high-K states is ≈ 3 times lower than for the low-K ones [9], by also the rotational damping width is $\approx 30\%$ reduced for high-K states (see Section 3) [16].

The rather low value $r = 0.2$ typically obtained for the low-K *versus* low-K ridge analysis may be understood from the fact that at most one or two E1 transitions cool the nucleus from the excited unresolved bands below $\approx$ 1 MeV of thermal energy. Such a modest cross talk between regular rotational bands is even more hindered among low-K and high-K states, as testified by the $\approx$0 correlation coefficients shown in figure 5(b). On the contrary, going up in heat energy, as probed by the transitions in the valley, the K-selection rule are expected to be weaken due to the K-mixing of the states. In fact, the somewhat larger values of the correlation coefficients measured for high-K *versus* low-K (panel 5(d)) as compared to low-K *versus* low-K (panel 5(c)) strongly suggest a gradual mixing of low and high-K configurations, giving rise to a larger number of common paths. The present picture well agrees with the theoretical predictions from the band mixing model on ^{163}Er [9], for which only above 2.5 MeV thermal energy the limit of strong K-mixing is achieved.

5. Conclusions

The γ-decay from the thermally excited rapidly rotating ^{163}Er nucleus is used to investigate the properties of the nuclear system up to $\approx$4 MeV of excitation energy above yrast. Two topics have been discussed. First, a direct experimental measurement of both compound and rotational damping widths Γ_μ and $\Gamma_{\rm rot}$ has been given, providing values of $\Gamma_{\rm rot} \approx 200$ keV and $\Gamma_\mu \approx 20$ keV for the angular momentum region $I \approx 30$–$40\hbar$ and internal excitation energy $U \approx 1.4$ MeV.

Secondly, the transition between order and chaos has been investigated in terms of persistence of selection rules on the K-quantum number. From a statistical analysis of γ–γ matrices gated by specific low-K/high-K discrete bands, a clear difference in the mixing process between low-K and high-K states is observed, as also suggested by the theory. In particular, for the lower interval $U < 1.2$ MeV, a rather strict conservation of the K-quantum number is found, while at higher internal energy (up to $U \approx 2.5$ MeV), the K-quantum number appears to be only partially conserved.

In both cases the experimental findings are in good agreement with band mixing calculation for ^{163}Er, providing a consistent picture of the rotational motion at finite temperature.

The work has been supported by the Italian Institute of Nuclear Physics, by the Danish Natural Science Foundation Research Council, by the Polish State Committee for Scientific Research (KBN) Grant No. 2 P03B 118 22, by EU Transnational Access to Major Research Infrastructures (Contract No. HPRI-CT-1999-00078) and by the EU TMR project (Contract No. ERBFMRXCT970123).

REFERENCES

[1] A. Bracco, S. Leoni, *Rep. Prog. Phys.* **65**, 299 (2002).
[2] M. Matsuo *et al.*, *Nucl. Phys.* **A620**, 296 (1997).
[3] S. Åberg, *Phys. Rev. Lett.* **64**, 3119 (1990).
[4] T. Døssing *et al.*, *Phys. Rep.* **268**, 1 (1996).
[5] S. Leoni *et al.*, *Nucl. Phys.* **A671**, 71 (2000).
[6] M. Matsuo *et al.*, *Nucl. Phys.* **A617**, 1 (1997).
[7] P. Bortignon, A. Bracco, R.A. Broglia, *Nuclear Structure at Finite Temperature*, Harw. Ac. Pub. 1998.
[8] M. Matsuo *et al.*, *Phys. Lett.* **B465**, 1 (1999).
[9] M. Matsuo *et al.*, *Nucl. Phys.* **A736** (2004) 241.
[10] G.B. Hagemann *et al.*, *Nucl. Phys.* **A618**, 199 (1997).
[11] D.C. Radford, *Nucl. Instrum. Methods* **A361**, 297 (1995).
[12] M. Matsuo *et al.*, *AIP Conf. Proc.* **656**, 32 (2003).
[13] A. Bracco *et al.*, *Phys. Rev. Lett.* **76**, 4484 (1996).
[14] P. Walker *et al.*, *Phys. Lett.* **B408**, 242 (1997).
[15] F.G. Kondev *et al.*, *Nucl. Phys.* **A632**, 473 (1998).
[16] S. Leoni, *Phys. Rev. Lett.* **93**, 022501 (2004).
[17] S.H. Sie *et al.*, *Phys. Rev. Lett.* **46**, 406 (1981).
[18] B.R. Mottelson, *Nucl. Phys.* **A557**, 717c (1993).
[19] I. Huseby *et al.*, *Phys. Rev.* **C55**, 1805 (1997).
[20] V.G. Soloviev, *Phys. Lett.* **B317**, 501 (1993).